Proceedings of the
Annual Stability Conference
Structural Stability Research Council
Baltimore, Maryland, April 10-13, 2018

Creep Buckling of Steel Beam-Columns Subjected to Fire

Mohammed A. Morovat[1], Michael D. Engelhardt[2], Todd A. Helwig[3]

Abstract
This paper presents highlights of a computational study to investigate the influence of thermal creep of steel on the ultimate strength of steel beam-columns at elevated temperatures. W12×120 wide flange beam-columns with the unsupported length of 240 inches are used in the simulations. A Pin-pin end-support condition, and an initial geometric imperfection having the shape of the first buckling mode with the amplitude of L/1000 formed the geometric boundary conditions. Beam-columns are subjected to a single end-moment, and are bent about the weak axis of their cross section. Thermal creep of steel is modeled following equations proposed by Fields and Fields for the creep of ASTM A36 steel. Thermal restraints, both axial and rotational, were ignored in the analyses. Representative results from creep buckling tests simulated at 500 °C are presented and discussed. Presentation of the results in the form of *Creep Buckling Curves* and *Isochronous Strength Interaction Curves* are proposed to quantify the effects of axial loads and end-moments on the time- and temperature-dependent behavior of steel beam-columns. Results from creep buckling simulations presented in this paper indicate that the combination effect of axial loads and end-moments have a significant impact on the predictions of the time-dependent ultimate strength of steel beam-columns subjected to fire.

1. Introduction
The strength and deformation capacities of steel beam-columns subjected to fire are influenced by many factors. One of the critical factors affecting the behavior of steel beam-columns in fire is the thermal creep of structural steel. Defined as time-dependent inelastic deformation, thermal creep results in degradation of the strength of steel at elevated temperatures. Further, thermal creep of steel results in additional deflection of beam-columns, and as a result, additional moment. Consequently, the behavior of steel beam-columns at elevated temperatures is governed by a phenomenon termed creep buckling, where the buckling capacity of a steel beam-column depends on the duration of applied loads and moments in addition to the slenderness and temperature. The effect of thermal creep of steel on the buckling behavior of steel beam-columns exposed to fire is therefore of particular importance, and it is not well understood and clearly treated in building codes and standards.

[1] Research Scientist Associate, University of Texas at Austin, <morovatma@utexas.edu>
[2] Professor, University of Texas at Austin, <mde@mail.utexas.edu>
[3] Professor, University of Texas at Austin, <thelwig@mail.utexas.edu>

The analysis of the buckling behavior of steel beam-columns at room temperature is very well documented in the literature on the stability of steel beam-columns (Ziemian 2010). However, literature on the buckling capacity of steel beam-columns exposed to fire temperatures is quite meager (Huang and Tan 2004; Knobloch et al. 2008; kodur and Dwaikat 2009; Choe et al. 2011; Morovat 2014). Specifically, there is very little study on the effect of thermal creep of steel on the buckling behavior of steel beam-columns when subjected to fire (Huang and Tan 2004; kodur and Dwaikat 2009; Li and Zhang 2012; Morovat et al. 2013; Morovat 2014). The time-dependent or creep behavior of steel beam-columns exposed to fire is therefore not well understood and clearly treated in building codes and standards including Eurocode 3 (2003) and the AISC Specification (2010).

To develop a better understanding of the effect of creep of steel on the buckling behavior of steel beam-columns at elevated temperatures, the authors performed a series of creep buckling simulations, highlights of which are presented in this paper. Some details about buckling tests simulated in Abaqus will first be provided. Results from both short-time and creep buckling tests on W12×120 wide flange columns under different combination of axial forces and end-moments at 500 °C are then presented and discussed. Conceptual representations of the results of the creep buckling tests in the form of *Creep Buckling Curves* and *Isochronous Strength Interaction Curves* are further proposed to better understand and quantify the effects of axial loads and end-moments on the time- and temperature-dependent behavior of steel beam-columns.

2. Simulations of Creep Buckling Tests on Beam-Columns: General Considerations

This section provides general information on the geometry and boundary conditions of the beam-columns considered in this study. Modeling the time-dependent behavior of the beam-column material as well as analysis schemes adopted to study the time-dependent behavior of steel beam-columns are also presented and discussed.

2.1 Geometry and Boundary Conditions

W12×120 wide-flange beam-columns with the unsupported length of 240 inches were utilized in the study. A Pin-pin end-support condition, and an initial geometric imperfection having the shape of the first buckling mode with the amplitude of L/1000 formed the geometric boundary conditions. As further indicated in Fig. 1, a concentric axial force P and a moment M applied at one end constituted the loading boundary conditions for the beam-columns. The end moment M was applied about the weak axis of the beam-column cross section. In addition, the beam-columns were modeled as 3D hexahedral eight-node linear brick elements (*C3D8R*) to conduct creep-buckling simulations in Abaqus.

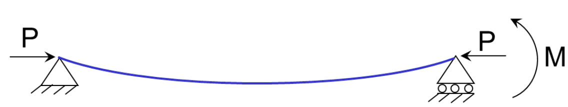

Figure 1: Pin-Pin Beam-Columns with a Moment Applied at One End

2.2 Time-Dependent Behavior of Structural Steel

Beam-columns were assumed to be made of ASTM A36 structural steel. As shown in Fig. 2, the time-independent inelastic behavior of ASTM A36 steel at elevated temperatures was modeled as an idealized elastic-plastic stress-strain relationship. The essential parameters of this model (i.e. elastic modulus and yield stress) were obtained at elevated temperatures using retention factors from Eurocode 3 (Eurocode 3 2006). As further presented in Fig. 2, the time-dependent or creep of structural steel was assumed to cause material nonlinearities in the knee region of stress-strain curves, and therefore, was modeled separately.

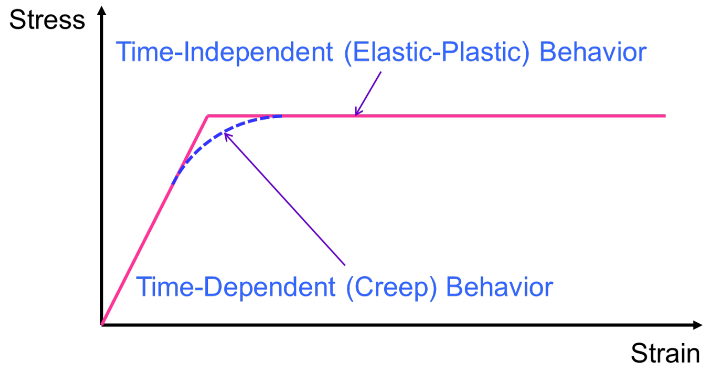

Figure 2: Conceptual Modeling of Time-Dependent Stress-Strain Behavior of Structural Steel at Elevated Temperatures

The time-dependent or creep behavior of ASTM A36 steel at elevated temperatures was defined using the model developed by Fields and Fields (1989) based on material tests by Skinner (1972). The creep model proposed by Fields and Fields (1989) incorporates a power law and represents creep strain, ε_c, in the form of a Norton-Bailey (Norton 1929; Bailey 1929) equation as follows:

$$\varepsilon_c = a t^b \sigma^c \tag{1}$$

In this equation, t is time and σ is stress. The parameters a, b and c are temperature-dependent material properties. Fields and Fields (1989) derived equations for these temperature-dependent material properties for ASTM A36 steel. The model developed by Fields and Fields (1989) is capable of predicting creep in the temperature range of 350 °C to 600 °C and for creep strains up to 6-percent. Note that the strain-hardening format of the power law creep shown in Eq. 1 was incorporated in the beam-column simulations (Morovat 2014). The strain hardening formulation was adopted to better represent the creep behavior of structural steel under variable stress conditions (stress redistribution in structural members).

2.3 Buckling Analysis Method

To study the effect of thermal creep of steel on the ultimate strength of steel beam-columns at elevated temperatures, two types of buckling tests were simulated in Abaqus. These two column tests are referred to in this paper as *Short-Time Buckling Tests* and as *Creep Buckling Tests*. Short-time buckling tests were simulated to characterize the time-independent strength of steel beam-columns at elevated temperatures. To obtain the time-independent or short-time buckling loads in Abaqus, inelastic load-deflection (or moment-rotation) analyses, using a nonlinear analysis scheme called Riks, were performed under the steady-state temperature conditions. Following the short-time buckling tests, creep buckling tests were simulated to characterize the time-dependent strength of steel beam-columns at elevated temperatures. In creep buckling simulations, temperature was first increased to the desired level, and then an axial force (a fraction of the ultimate load predicted in the short-time buckling test) combined with an end-moment (a fraction of the plastic moment of the cross section) was applied to the column. No material creep was considered in these two steps. Next, incorporating a nonlinear analysis scheme called Visco, the beam-column was allowed to creep over the time period of 6 hours under the sustained axial load and end moment. Finally, the time-to-buckle due to creep was estimated. Note that, to model initial geometric imperfections in both column tests, eigen-value buckling analyses were performed. The initial shape of the beam-column was taken as the shape of the first buckling mode, and the magnitude of the imperfection was L/1000.

3. Simulations of Creep Buckling Tests on Beam-Columns: Results and Discussions

The two types of beam-column buckling simulations introduced above were used to examine the effect of creep of steel on the buckling behavior of steel beam-columns at elevated temperatures of fire. Specifically, the effect of an end-moment in reducing the time-dependent buckling strength of steel columns at elevated temperatures is presented and discussed in this section.

3.1 Time-Dependent Behavior of Beam-Columns

The time-depending behavior of steel columns in the presence of an end-moment can be studied by conducting a series of creep buckling tests either under a constant end moment and different axial loads, or under a constant axial force and different end-moments. For instance, Fig. 3 shows representative results from three creep buckling tests at 500 °C simulated for a specific end moment of 599.5 kip-in., which is about 25% of the plastic moment of the column cross-section (M_P). The results are presented in Fig. 3 as plots of lateral deflection (at the point of maximum displacement) versus time at different axial load levels. Fig. 3 clearly shows that the rate of change of deflection with time increases very slowly at the beginning and then increases more rapidly until the column no longer can support its load (end-moment combined with an axial load). The time at which the displacement-time curves become nearly vertical after entering the tertiary stage is considered the *failure time* or *time-to-buckle*. As further depicted in Fig. 3, the presence of a small end-moment of 599.5 kip-in. resulted in deflected shapes very similar to those of the corresponding column subjected to axial loads only. In other words, the time-dependent behavior of beam-columns shown in Fig. 3 closely follows that of the corresponding columns.

Fig. 4 further represents sample results from three creep buckling tests at 500 °C simulated for a specific axial load of 285.6 kips, which is about 40% of the time-independent buckling capacity of the corresponding column (P_{cr} = 714 kips at 500 °C). The results are again shown in Fig. 4 as plots of lateral deflection (at the point of maximum displacement) versus time at different end-moment levels. In addition, like Fig. 3, Fig. 4 shows the same trend in deflection changes with time where the rate of change of deflection with time increases very slowly at the beginning and then increases more rapidly until the column no longer can support its load (end-moment combined with an axial load). However, the *failure time* or *time-to-buckle* for the beam-columns in Fig. 4 takes place as soon as the displacement-time curves enter the tertiary stage. More specifically, higher end-moments applied to beam-columns in Fig. 4 resulted in more rapid failure of beam-columns compared to those in Fig. 3. Additionally, these higher end-moments changed the deflected shape of the column as shown in Fig. 4.

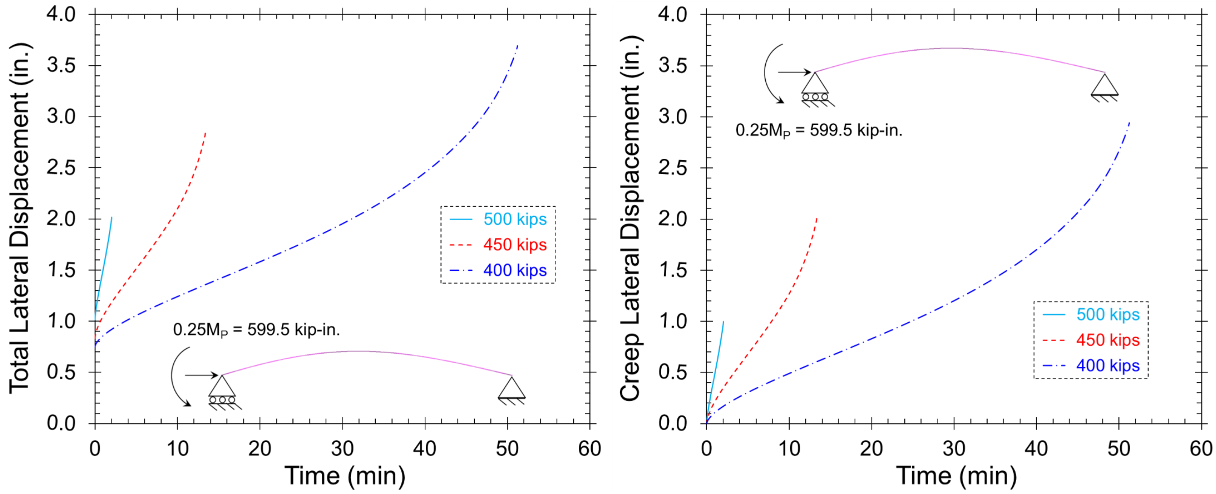

(a) Total Deflection (b) Time-Dependent Deflection

Figure 3: Representative Results of Creep Buckling Tests on Steel Beam-Columns at 500 °C: Applied End-Moment of 599.5 kip-in. Combined with Different Axial Loads

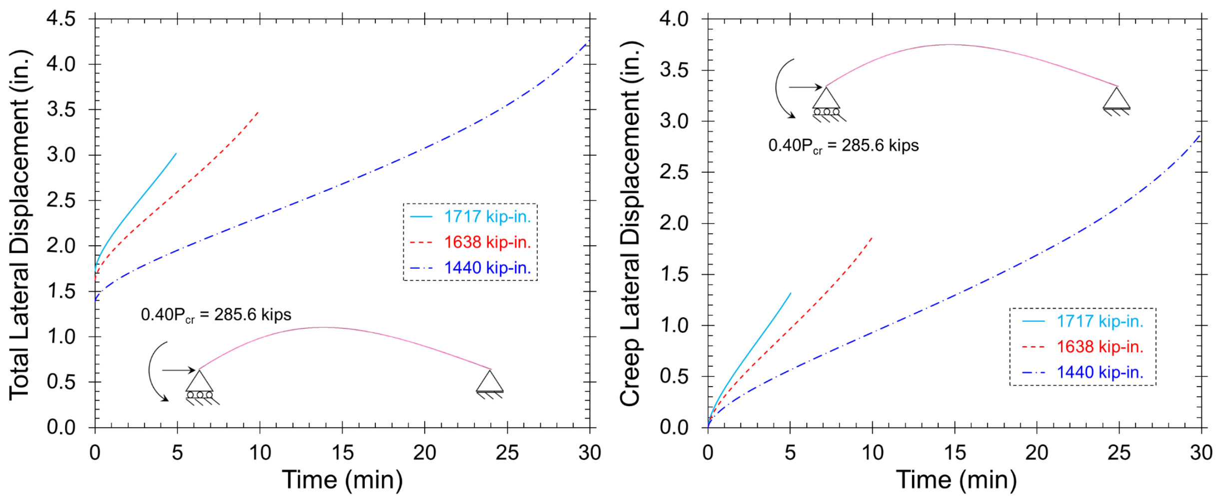

(a) Total Deflection (b) Time-Dependent Deflection

Figure 4: Representative Results of Creep Buckling Tests on Steel Beam-Columns at 500 °C: Applied Axial Load of 285.6 kips. Combined with Different End-Moments

3.2 Effect of End-Moments

Creep test results, shown in Figs. 3 and 4 above, clearly indicate that the magnitude of end-moments can affect the predictions of the creep buckling strength of steel beam-columns in fire. To better understand the effect of end-moments on the time-dependent response of steel columns at elevated temperatures, the time-dependent behavior of two columns (subjected to axial loads only) are evaluated and compared to that of the corresponding beam-column subjected to an end-moment of 1440 kip-in. (Fig. 4). The first column was subjected to an axial load of 285.6 kips, equal to the axial load applied to the beam-column subjected to an end-moment of 1440 kip-in. The second column was subjected to an axial load of 531.6 kips that resulted in the failure time of 30-minutes, equal to the failure time of the beam-column subjected to an end-moment of 1440 kip-in. The time-dependent buckling behaviors of these two columns are presented in Figs. 5 and 6, respectively. As seen in Fig. 5, the time-to-failure for the column subjected to axial load of 285.6 kips and no end-moment increased significantly to about 18,000-minutes. Further, the fundamental shape of the deflection-time curve for this column also changed in that the failure occurred when the displacement-time curve was dominated by the tertiary stage, and that the primary stage was almost disappeared. For the second column subjected to a larger axial load of 531.6 kips (shown in Fig. 6), the time-dependent behavior is more similar to that of the beam-column subjected to an end-moment of 1440 kip-in. (Fig. 4). Again, the primary stage is less pronounced in the deflection-time behavior of the column (Fig. 6) as compared to that of the beam-column shown in Fig. 4.

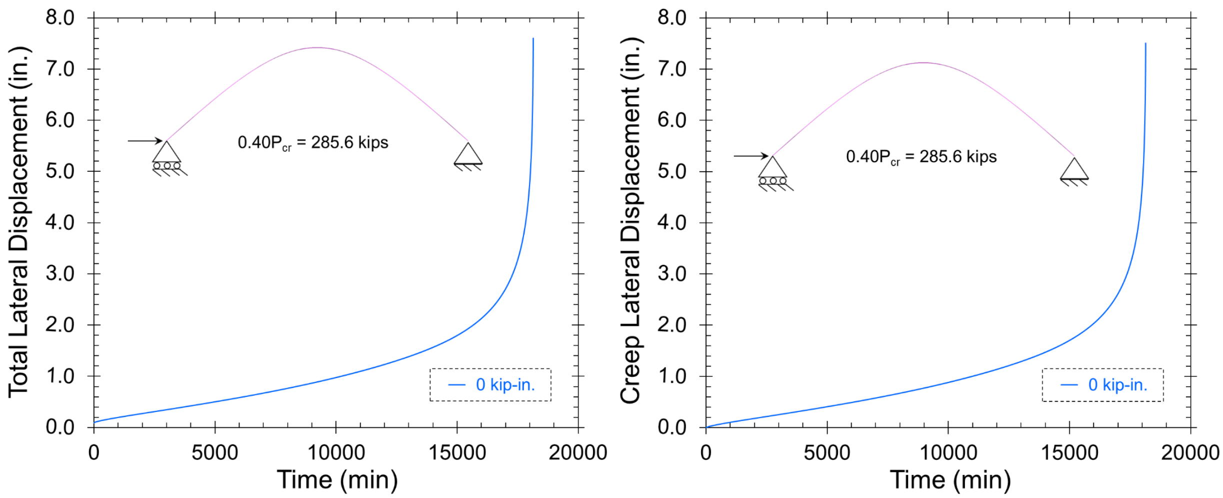

(a) Total Deflection (b) Time-Dependent Deflection
Figure 5: Representative Results of Creep Buckling Tests on Steel Beam-Columns at 500 °C: Applied Axial Load of 285.6 kips. with No End-Moments

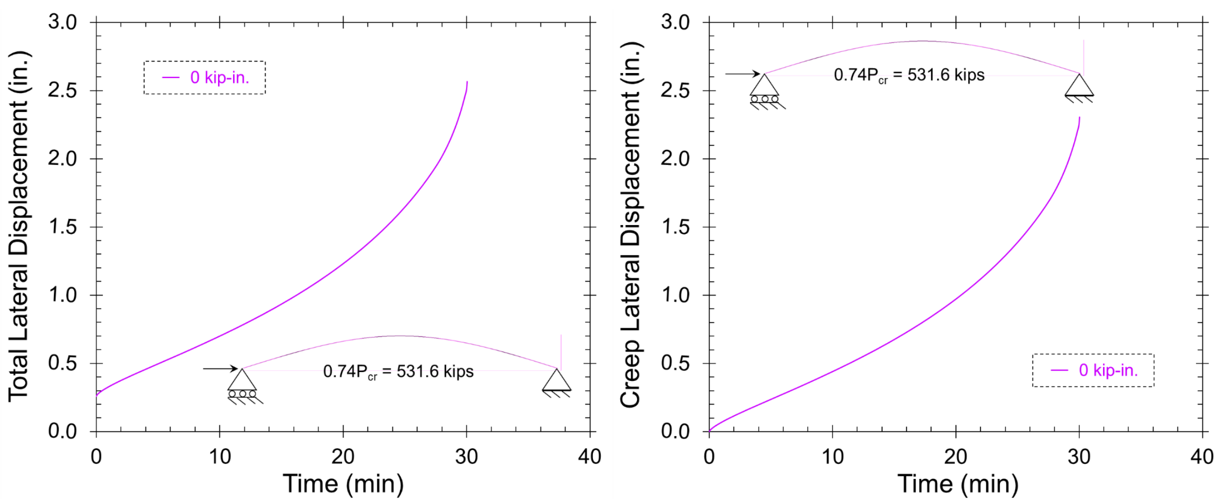

(a) Total Deflection (b) Time-Dependent Deflection
Figure 6: Representative Results of Creep Buckling Tests on Steel Beam-Columns at 500 °C: Applied Axial Load of 531.6 kips. with No End-Moments

The effect of end-moments on the creep buckling behavior of steel beam-columns can further be investigated by studying the time-dependent stress distributions over the column cross-section. The creep-induced stresses during the creep buckling tests on the above-discussed columns are shown in Figs. 7, 8 and 9. It can again be observed from Figs. 7, 8 and 9 that the presence of an end-moment (Fig. 7) results in more pronounced primary and less dominated tertiary stages in the time-dependent stress distributions on the tension side of the column cross-section. This is a very important observation since the time-dependent internal moment generated at the section of maximum lateral displacement during a creep-buckling test closely follows the stress distributions on the tension side of the column cross-section. The corresponding time-dependent section moments during creep buckling tests are illustrated in Figs. 10, 11 and 12. In addition, as indicated in Fig. 7(a), combined effects of an axial load and an end-moment may result in yielding of the compression side of the column cross-section at the beginning of the creep buckling test. Therefore, the presence of an end-moment causes the stresses to relax with time on the compression side during a creep buckling test. The stress relaxation of compressive stresses results in an increase in stresses on the tension side of the column cross-section and therefore can significantly reduce the buckling life of steel beam-columns at elevated temperatures.

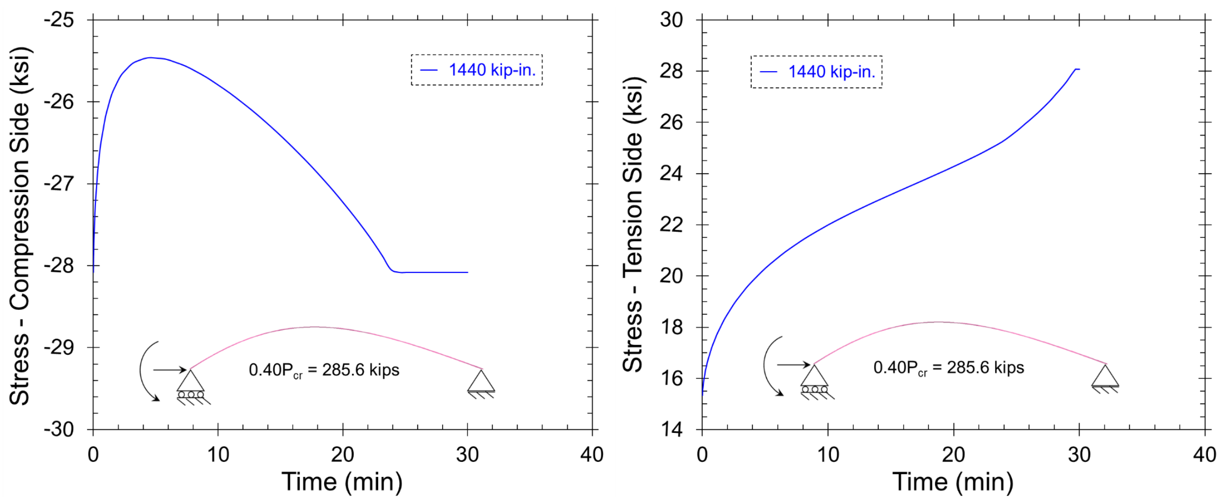

(a) Compression Side (b) Tension Side

Figure 7: Time-Dependent Stresses during a Creep Buckling Test on a Steel Beam-Column at 500 °C: Applied Axial Load of 285.6 kips. Combined with an End-Moment of 1440 kip-in.

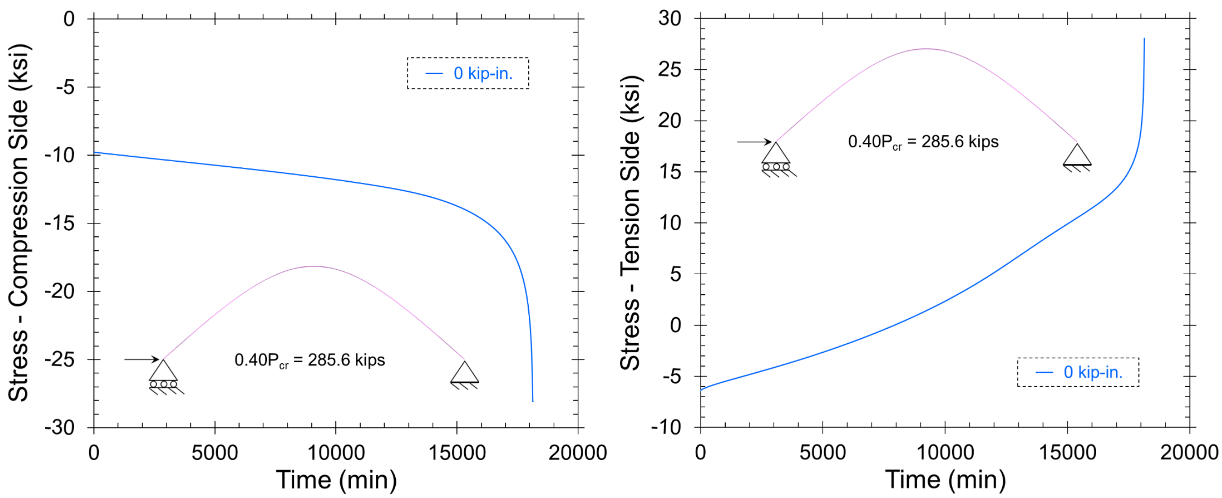

(a) Compression Side (b) Tension Side

Figure 8: Time-Dependent Stresses during a Creep Buckling Test on a Steel Column at 500 °C: Applied Axial Load of 285.6 kip-in. with No End-Moments

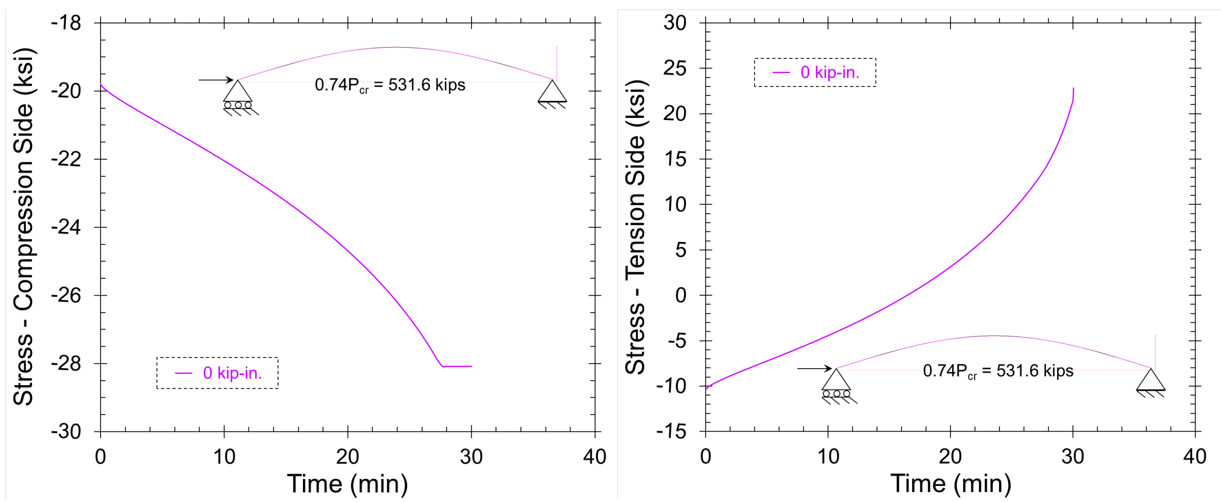

(a) Compression Side (b) Tension Side

Figure 9: Time-Dependent Stresses during a Creep Buckling Test on a Steel Column at 500 °C: Applied Axial Load of 531.6 kip-in. with No End-Moments

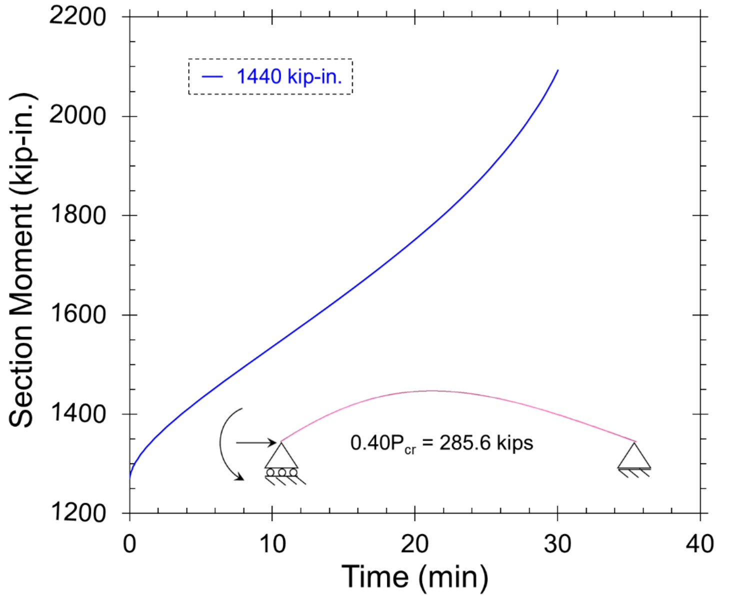

Figure 10: Time-Dependent Section Moments during a Creep Buckling Test on a Steel Beam-Column at 500 °C: Applied Axial Load of 285.6 kips. Combined with an End-Moment of 1440 kip-in.

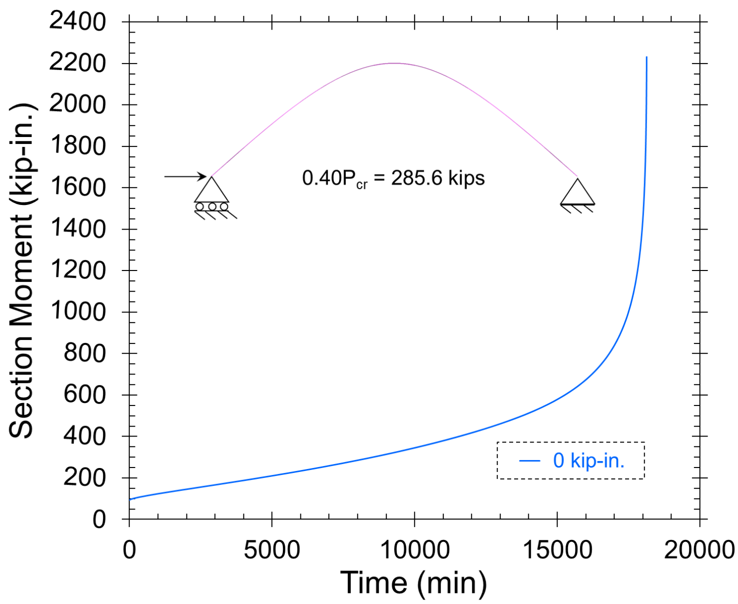

Figure 11: Time-Dependent Section Moments during a Creep Buckling Test on a Steel Column at 500 °C: Applied Axial Load of 285.6 kip-in. with No End-Moments

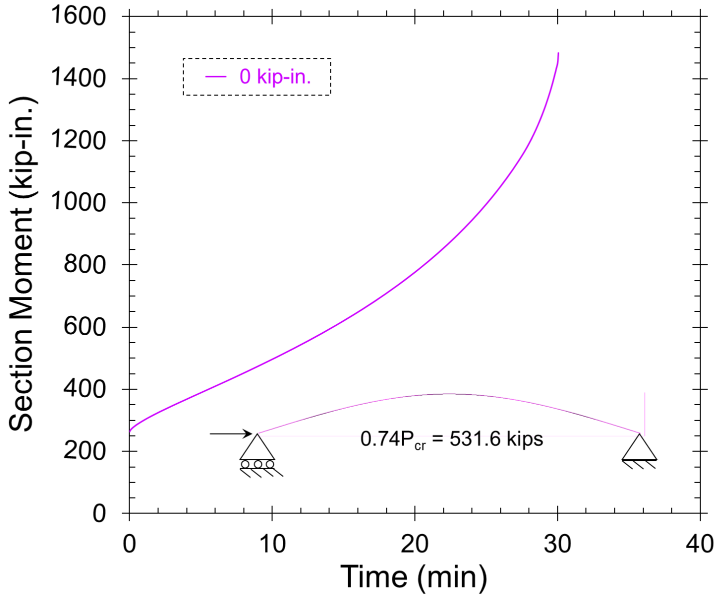

Figure 12: Time-Dependent Section Moments during a Creep Buckling Test on a Steel Column at 500 °C: Applied Axial Load of 531.6 kip-in. with No End-Moments

4. Time- and Temperature-Dependent Strength of Beam-Columns

The results from creep buckling tests presented in Section 3 clearly demonstrate that the ultimate strength of steel beam-columns at elevated temperatures changes with time. Therefore, using the results of creep buckling tests, samples of which presented in Figs. 3 and 4, the buckling strength of steel beam-columns can be explicitly defined as a function of time. As will be explained and discussed in the following, the time- and temperature-dependent behavior of steel beam-columns can be represented using the concepts of *Creep Buckling Curves* and *Isochronous Strength Interaction Curves*.

4.1 Creep Buckling Curves

The displacement-time curves from creep buckling tests at elevated temperatures (like those presented in Fig. 3 at 500 °C) can be used to construct time-dependent buckling curves for steel beam-columns. Examples of such curves that are referred herein as *Creep Buckling Curves* are shown in Fig. 13 (a) for the temperature of 500 °C. In Fig. 13 (a), time effects on the buckling behavior of steel beam-columns are depicted as plots of buckling moment versus time for different axial load levels. Therefore, each point on these curves represents a creep buckling test simulated in Abaqus, and as a result, values on the time axis are indicative of *failure time* or *time-to-buckle*. Further, results from short-time buckling simulations are indicated as buckling moments at time zero on the creep buckling curves in Fig. 13 (a). As expected and seen in Fig. 13 (a), the column axial load has detrimental impact on the time-dependent strength of beam columns at the elevated temperature of 500 °C. Therefore, as the column axial load decreases, the behavior of beam-columns is governed by the yielding and therefore is less influenced by the thermal creep of steel (note that the yield stress of steel is assumed time-independent in this study).

To better gauge the effect of column axial loads on the time-dependent response of steel beam-columns at elevated temperatures, creep buckling curves in Fig. 13 (a) are normalized with respect to the corresponding short-time buckling moments and replotted in Fig. 13 (b). As seen more clearly in Fig. 13 (b), the buckling capacity of beam-columns with larger axial loads is more affected by the thermal creep of steel at the representative temperature of 500 °C.

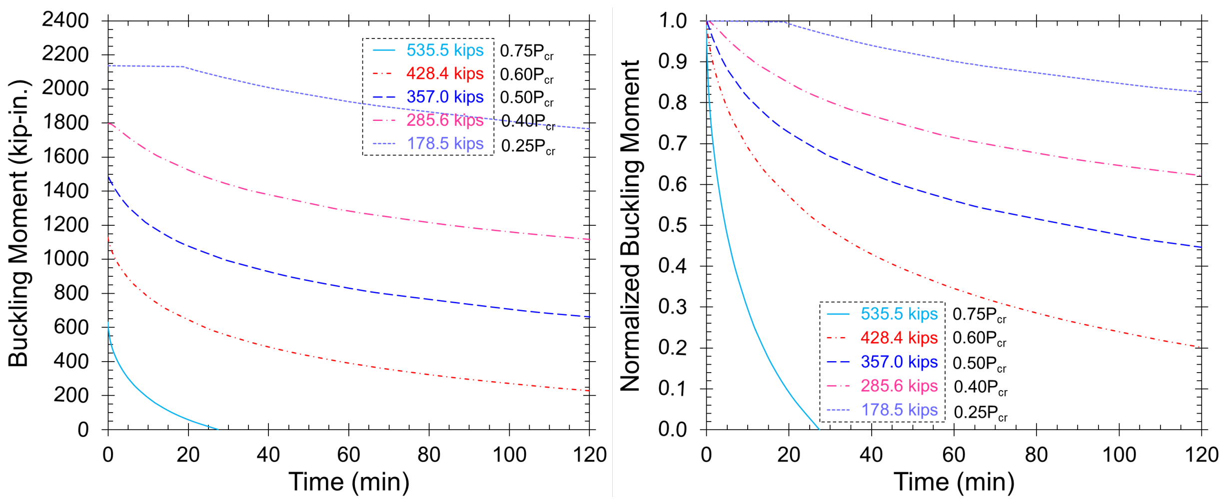

(a) Buckling Curves (b) Normalized Buckling Curves

Figure 13: Representative Creep Buckling Curves for Steel Beam-Columns at 500 °C: Buckling Moment versus Time for Different Column Axial Loads

Similar to the developments described above and presented in Fig. 13 (a), curves like those shown in Fig. 4 at 500 °C can be used to construct *Creep Buckling Curves*, where time effects on the buckling behavior of steel beam-columns are illustrated as plots of buckling load versus time for different end-moment levels. Representatives of such curves are illustrated in Fig. 14 (a) for the temperature of 500 °C. Again, each point on the curves in Fig. 14 (a) represents a creep buckling test simulated in Abaqus, and as a result, values on the time axis are indicative of *failure time* or *time-to-buckle*. In addition, results from short-time buckling simulations are indicated as buckling loads at time zero on the creep buckling curves in Fig. 14 (a).

To better understand the effect of column end-moments on the time-dependent response of steel beam-columns at elevated temperatures, creep buckling curves in Fig. 14(a) are normalized with respect to the corresponding short-time buckling loads and replotted in Fig. 14 (b). As observed in Fig. 14(b), the effect of end-moments on the creep buckling capacity of steel beam-columns is a complicated phenomenon. This is the case since for buckling times less than about 45 minutes, the ultimate strength of beam-columns subjected to larger end-moments is less affected by the thermal creep of steel at the representative temperature of 500 °C. However, when subjected to larger end-moments and exposed to fire-temperature durations longer than 45 minutes, the buckling capacity of steel beam-columns becomes highly time dependent at 500 °C.

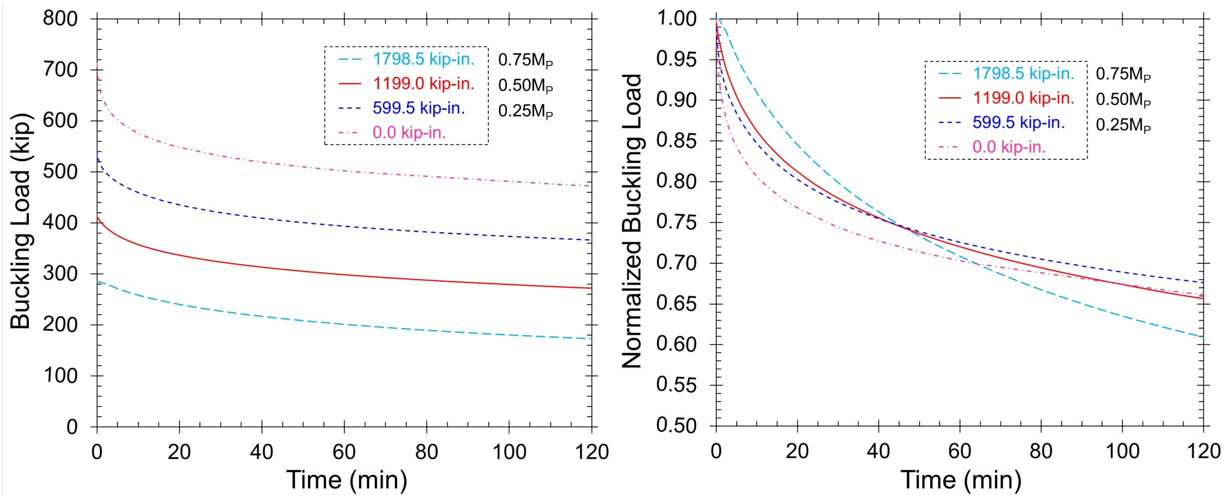

(a) Buckling Curves (b) Normalized Buckling Curves

Figure 14: Representative Creep Buckling Curves for Steel Beam-Columns at 500 °C: Buckling Load versus Time for Different Column End-Moments

4.2 Isochronous Strength Interaction Curves

Time effects on the buckling capacity of steel beam-columns can alternatively be illustrated in the form of *Isochronous Strength Interaction Curves*, a sample of which depicted in Fig. 15. Fig. 15 basically presents a series of axial force-moment (P-M) Interaction isochrones for Pin-Pin Beam-Columns at 500 °C. Each isochrone represents a strength interaction curve corresponding to a specific buckling time. Consequently, the isochronous strength interaction curves in Fig. 15 can be used to predict the time-dependent ultimate strength of steel beam-columns at 500 °C for any combinations of axial forces and end-moments.

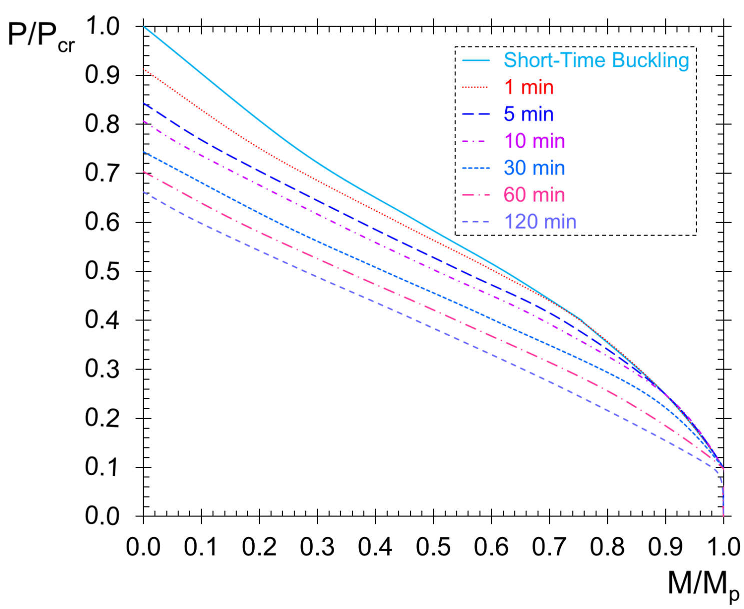

Figure 15: Isochronous Axial Force-Moment (P-M) Interaction Curves for Pin-Pin Beam-Columns at 500 °C

5. Conclusion

Highlights of an extensive computational study conducted by the authors to investigate the effect of creep of steel on the buckling behavior of steel beam-columns subjected to fire were presented in this paper. Both time-independent and creep buckling tests on W12×120 wide flange beam-columns under the pin-pin boundary condition were simulated in Abaqus to characterize short-time and creep buckling loads and moments at elevated temperature of 500 °C.

The results from creep buckling simulations indicate that the column axial loads combined with end-moments have a significant impact on the predictions of the creep strength of steel beam-columns subjected to fire. Representations of the time- and temperature-dependent behavior of steel beam-columns in the forms of *Creep Buckling Curves* and *Isochronous Strength Interaction Curves* help to better understand and quantify the effects of axial loads and end-moments on the overall stability of steel beam-columns subjected to fire temperatures.

Acknowledgments

The research reported herein was conducted as part of research projects on *Elevated Temperature Performance of Beam End Framing Connections*, on *Creep Buckling of Steel Columns Subjected to Fire* and on *Elevated Temperature Performance of Shear Connectors for Composite Beams*, all supported by the National Science Foundation (NSF Awards 0700682, 0927819 and 1031099, respectively). The support of the National Science Foundation and of the former NSF Program Directors M.P. Singh and Douglas Foutch is gratefully acknowledged. Any opinions, findings, and conclusions or recommendations expressed in this paper are those of the authors and do not reflect the views of the National Science Foundation.

References

American Institute of Steel Construction (AISC). (2010). *Specification for Structural Steel Buildings*, Standard ANSI/AISC 360-10, Chicago.

Bailey, R.W. (1929). "Creep of Steel under Simple and Compound Stress." *Engineering*, 148, 121, 528-529.

Choe, L., Varma, A.H., Agarwal, A., and Surovek, A. (2011). "Fundamental Behavior of Steel Beam-Columns and Columns under Fire Loading: Experimental Evaluation." *Journal of Structural Engineering, ASCE*, 137(9) 954-966.

Eurocode 3 (2006). *Design of Steel Structures. Part 1-2: General rules. Structural Fire Design*, EN 1993-1-2 European Committee for Standardization, CEN.

Fields, B.A., and Fields, R.J. (1989). *Elevated Temperature Deformation of Structural Steel*, Report NISTIR 88-3899, NIST, Gaithersburg, MD.

Huang, Z.-F., and Tan, K.-H. (2004). "Effects of External Bending Moments and Heating Schemes on the Responses of Thermally Restrained Steel Columns." *Engineering Structures*, 26 769-780.

Knobloch, M., Fontana, M., and Frangi, A. (2008). "Fire Resistance of Steel Beam-Columns Subjected to Axial Compression and Biaxial Bending with Non-Uniform Bending Moment Distribution." *Proceedings of the Fifth International Conference on Structures in Fire (SiF'08)*, 56-67.

Kodur, V.K.R., and Dwaikat, M.M.S. (2009). "Response of Steel Beam-Columns Exposed to Fire." *Engineering Structures*, 31 369-379.

Li, G.-Q., and Zhang, C. (2012). "Creep Effect on Buckling of Axially Restrained Steel Columns in Real Fire." *Journal of Constructional Steel Research*, 71 182-188.

Morovat, M.A., Engelhardt, M.D., Helwig, T.A., and Taleff, E.M. (2013). "Influence of Creep on the Stability of Steel Columns Subjected to Fire," *Proceedings of the Annual Stability Conference,* Structural Stability Research Council, St. Louis, Missouri, April 16-20.

Morovat M.A. (2014). *Creep Buckling of Steel Columns Subjected to Fire*, Ph.D. Dissertation, Department of Civil, Architectural and Environmental Engineering, The University of Texas at Austin.

Norton, F.H. (1929). *The Creep of Steel at High Temperatures*, McGraw-Hill Book Company, Inc., New York.

Skinner, D.H. (1972). "Determination of High Temperature Properties of Steel." *Broken Hill Proprietary Company, Technical Bulletin*, 16(2) 10-21.

Ziemian, R.D. Editor (2010) *Guide to Stability Design Criteria for Metal Structures*, 6th Edition, John Wiley & Sons, Inc., New York